RSC Advances

ROYAL SOCIETY OF CHEMISTRY

www.rsc.org/advances

Table of Contents

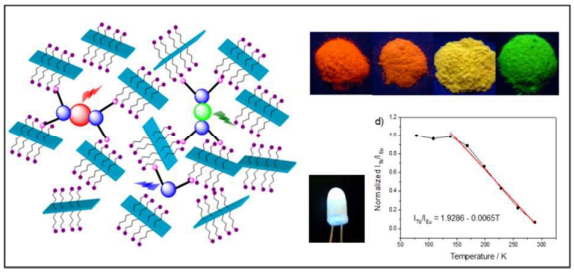

Lanthanide(III)-based multi-colored hybrid materials showing potential in WLED and self-referencing luminescent thermometer.

Cite this: DOI: 10.1039/cOxxOOOOOx

www.rsc.org/xxxxxx

PAPER

Multi-colored Luminescent Light-harvesting Hybrids Based on Aminoclay and Lanthanide Complexes†

Tianren Wang, Xiaoyan Yu, Zhiqiang Li, Jin Wang and Huanrong Li*

Received (in XXX, XXX) Xth XXXXXXXXX 20XX, Accepted Xth XXXXXXXXX 20XX

DOI: 10.1039/b000000x

Luminescent light-harvesting hybrids with tunable emission properties have been achieved by co-assembling lanthanide(III) cations, 2,2'-bipyridine-4,4'-dicarboxylic acid with molecular exfoliated aminoclay sheets in aqueous system at room temperature. Emission colors of the resulting materials can be fine tuned by varying the molar ratio of Eu^{3+} to Tb^{3+}, the excitation wavelength and the temperature. The AC-Bipy-Eu_1Tb_{99} exhibits an excellent co-ordinate of (0.30, 0.30) located in the "white region" of CIE 1931 chromaticity diagram (under 350 nm UV illumination). Interestingly, the emission intensity ratio of $^5D_4 \rightarrow {}^7F_5$ transition (Tb^{3+} of AC-Bipy-Tb) to $^5D_0 \rightarrow {}^7F_2$ transition (Eu^{3+} of AC-Bipy-Eu) can be linearly related to temperature from 138 to 288 K. Such luminescent properties make the materials good candidates for designing optoelectronic devices like white LED and self-referencing luminescent thermometers.

Introduction

Multicolored luminescent materials including red, green and blue (RGB) components as well as white-light emission based on trivalent lanthanide cations (Ln^{3+}) and organic sensitizer have attracted considerable interests in recent years and can be potentially utilized for manufacturing full-color displays, back-lighting or even the next-generation lighting tools. [1-6] Most of Ln^{3+} exhibit intriguing optical properties such as narrow emission bands, long lifetime and ligand-induced Stokes' shift, etc. [7-10] Coordination between Ln^{3+} and organic ligands resulting in the organic complexes is a typical way to achieve lanthanide luminescence on the basis of the well-known "antenna effect". [7] In particular, the trivalent europium cations (Eu^{3+}) and terbium cations (Tb^{3+}) are employed as the red and green emitters for the coordination systems, respectively, and the ligand with a triplet state energy level between 22000 and 27000 cm^{-1} can make both of them sensitized, [11, 12] which provides a possibility to achieve tunable luminescence through fine control of energy transfer process between just a single organic ligand and Ln^{3+}. [1] Emission color tuning has been observed in smartly designed lanthanide complexes where only part of the energy absorbed by the sensitizing fluorophore was transferred to Ln^{3+} ions. A consequence is that three components (red from Eu^{3+}, green from Tb^{3+} and blue from the fluorophore) occur simultaneously, and the achievement of the color tuning can be realized by changing the relative intensity of the three components. However, drawbacks such as low thermo- and photo- stability of the pure complexes as well as their complicated synthetic procedure severely limit their full exploitation in practical applications. [13] Hybridation of the organic complexes with thermo-stable substrates such as zeolite, [1, 14, 15] clay, [16-18] polyhedral oligomeric silsesquioxanes (POSS) [19, 20] or ionic liquids (ILs) [21, 22] to form organic-inorganic hybrid materials with enhanced optoelectronic and mechanical properties, as well as thermal-and photo-stability. Fascinatingly, tunable emission colors including white light have been observed in some of the organic-inorganic hybrid materials due to the partial energy transfer from the organic sensitizer to Ln^{3+} ions [1, 2, 23-25]. However, it remains a challengeable task to prepare the hybrid materials with tunable emission colors by using inexpensive raw materials as well as simple and environmentally friendly procedure.

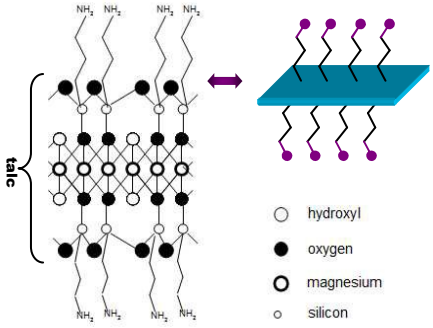

Figure 1. A single unit of aminoclay (AC), with a talc-like structure and an approximate composition of $R_8Si_8Mg_6O_{16}(OH)_4$ where R- is the aminopropyl pendent ($NH_2CH_2CH_2CH_2$-). [29]

Aminoclay (AC, Figure 1), a layered magnesium silicate covalently functionalized with amino groups, has proven to be the suitable inorganic component for preparing multicolored luminescent materials, since the single units of AC can be absolutely exfoliated in water due to the charge repulsion between protonated aminopropyl groups.[26] These positively charged, molecular exfoliated AC sheets can be co-assembled with blue emitting coronene tetracarboxylate salt and the green emitting perylene tetracarboxylate salt to result in highly transparent and luminescent gels.[27, 28] We recently prepared luminescent lanthanide-based organic-inorganic hybrid materials using this strategy by simple supramolecular co-assembly of AC, Sodium 1,2,4,5-benzenetetracarboxylate and Ln^{3+} (Ln=Eu, Tb, or Eu and Tb) in aqueous medium at room temperature. The luminescent materials display various emission colors including white light with good color purity and linear temperature-dependent luminescent behavior. [29] Because the preparing procedure for the materials is simple, environmentally friendly and less-time consuming, we therefore intend to extend our research to other organic ligand such as 2,2'-bipyridine-4,4'-dicarboxylic acid (we denote as H_2Bipydc).

H_2Bipydc has been extensively exploited for the sensitization of Ln^{3+} coupled with the remarkable ligand-to-metal energy transfer efficiency that has aroused our great interests, and such kind of works have also been developed by several groups. For instance, Calefi *et al.* [30] reported a class of Eu^{3+} and Tb^{3+} complexes by using the H_2Bipydc as the organic ligand. The dominant luminescence of Eu^{3+} ($^5D_0 \rightarrow {}^7F_2$) and Tb^{3+} ($^5D_4 \rightarrow {}^7F_5$) can both be observed. As a modified work, Li and co-workers [31] grafted the H_2Bipydc-Ln^{3+} complexes onto a silica sol-gel glass *via* Si-C covalent bonds, affording the materials improved stability and processibility and also provides a method to prepare lanthanide luminescent materials through sol-gel process. Unfortunately, the procedure of this work is still highly long time-consuming (about half a month). Herein we present novel supramolecular luminescent materials by co-doping of deprotonated H_2Bipydc, AC and Ln^{3+} in aqueous medium at room temperature.

Results and discussion

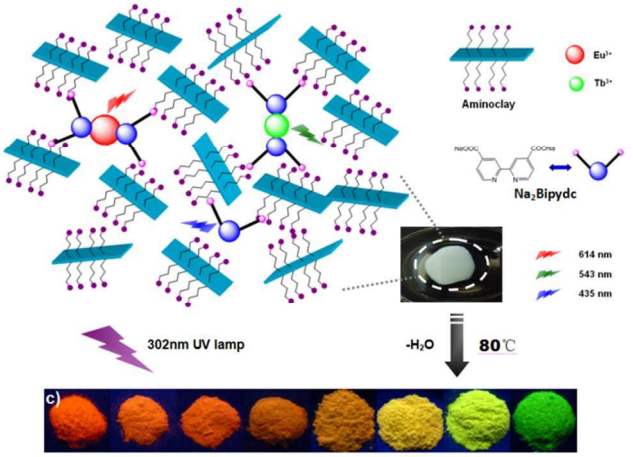

Scheme 1. a) Illustration of the predicted structure of the AC-Bipy-Ln hybrid luminescent materials. The molar ratio of the components is AC : Na_2Bipydc : $LnCl_3$ = 3.46 : 2 : 1; b) AC-Bipy-Ln hydrogel; c) luminescent powders of AC-Bipy-Eu, AC-Bipy-Eu_1Tb_1, AC-Bipy-Eu_1Tb_4, AC-Bipy-Eu_1Tb_{14}, AC-Bipy-Eu_1Tb_{24}, AC-Bipy-Eu_1Tb_{49}, AC-Bipy-Eu_1Tb_{99} and AC-Bipy-Tb, from left to right in the order, respectively (under 302 nm UV lamp illumination).

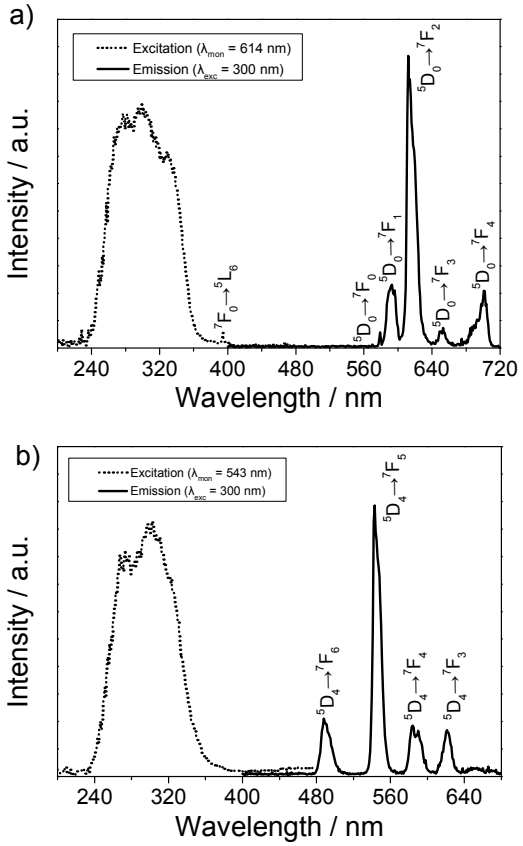

Figure 2. Luminescence spectra of a) AC-Bipy-Eu, the excitation spectrum (dot line) was obtained by monitoring the $^5D_0 \rightarrow {}^7F_2$ emission at 614 nm, and the emission spectrum (solid line) was obtained upon excitation at 300 nm; b) AC-Bipy-Tb, the excitation spectrum (dot line) was obtained by monitoring the $^5D_4 \rightarrow {}^7F_5$ emission at 543 nm, and the emission spectrum (solid line) was obtained upon excitation at 300 nm). All spectra were measured at room temperature.

The Na_2Bipydc (see Scheme 1a) was applied as the organic ligand for Ln^{3+}. The negatively charged carboxylate anions of which can interact electrostatically with the positively charged amino groups of AC in aqueous system [27] to result in a white

hydrogel (Scheme 1b) that we denote as AC-Bipy, which is easily coordinated with Ln^{3+} to form novel luminescent hydrogel named AC-Bipy-Ln (AC-Bipy-Eu, AC-Bipy-Tb and AC-Bipy-Eu_xTb_y, where the x/y represents the molar ratio of Eu^{3+} and Tb^{3+}). Luminescent powders of AC-Bipy-Ln with various emission colors and satisfied color purity (Scheme 1c) were further obtained after dehydration in air at 80 ℃ for several hours. Emission colors of the materials can be tuned by changing the molar ratio of Eu^{3+} and Tb^{3+}, excitation wavelength and temperature, as revealed by the luminescence data and the Commission Internationale de L'Eclairage (CIE) co-ordinates discussed afterwards.

The luminescence spectra of AC-Bipy-Eu and AC-Bipy-Tb were exhibited in Figure 2. A broad band between 240 and 400 nm attributed to the absorption of the bipyridine moieties is observed (Figure 2a). In addition, a much weaker sharp line at 395 nm ($^7F_0 \rightarrow {}^5L_6$ transition) assigned to the intra-configurational excitation of Eu^{3+} is observed, indicating that the Eu^{3+} are essentially excited by the ligand rather than by direct population of the intra-$4f^6$ energy levels. The emission spectrum of AC-Bipy-Eu exhibits five prominent lines, ascribed to the $^5D_0 \rightarrow {}^7F_J$ (J = 0, 1, 2, 3, 4) transitions of Eu^{3+}, with the red emission (Scheme 1c) of the $^5D_0 \rightarrow {}^7F_2$ transition as the dominant feature. AC-Bipy-Tb displays similar excitation spectrum (Figure 2b) to that of AC-Bipy-Eu, but no obvious f-f transitions of Tb^{3+} can be observed. Four sharp emission bands shown in Figure 2b are attributed to the $^5D_4 \rightarrow {}^7F_J$ (J = 6, 5, 4, 3) transitions of Tb^{3+}, which is dominated by the $^5D_4 \rightarrow {}^7F_5$ transition at 543 nm (green luminescence, see Scheme 1c). Tunable luminescence has been obtained by changing the molar ratio of Eu^{3+} and Tb^{3+} in AC-Bipy-Ln excited at 300 nm (Figure 3a, Figure 3c and Table S1). The $^5D_0 \rightarrow {}^7F_J$ (J = 0, 1, 2, 3, 4) transitions of Eu^{3+} and the $^5D_4 \rightarrow {}^7F_J$ (J = 6, 5, 4, 3) transitions of Tb^{3+} occur simultaneously in Figure 3a, suggesting that the bipyridine moieties are able to sensitize both Eu^{3+} and Tb^{3+} concurrently in AC-Bipy-Eu_xTb_y. With the decrease of molar ratio of Eu^{3+} and Tb^{3+}, the relative emission intensity of Eu^{3+} and Tb^{3+} reduces consistently, leading to a series of the emission colors from red to green through orange and yellow (see Scheme 1c and Figure 3c).

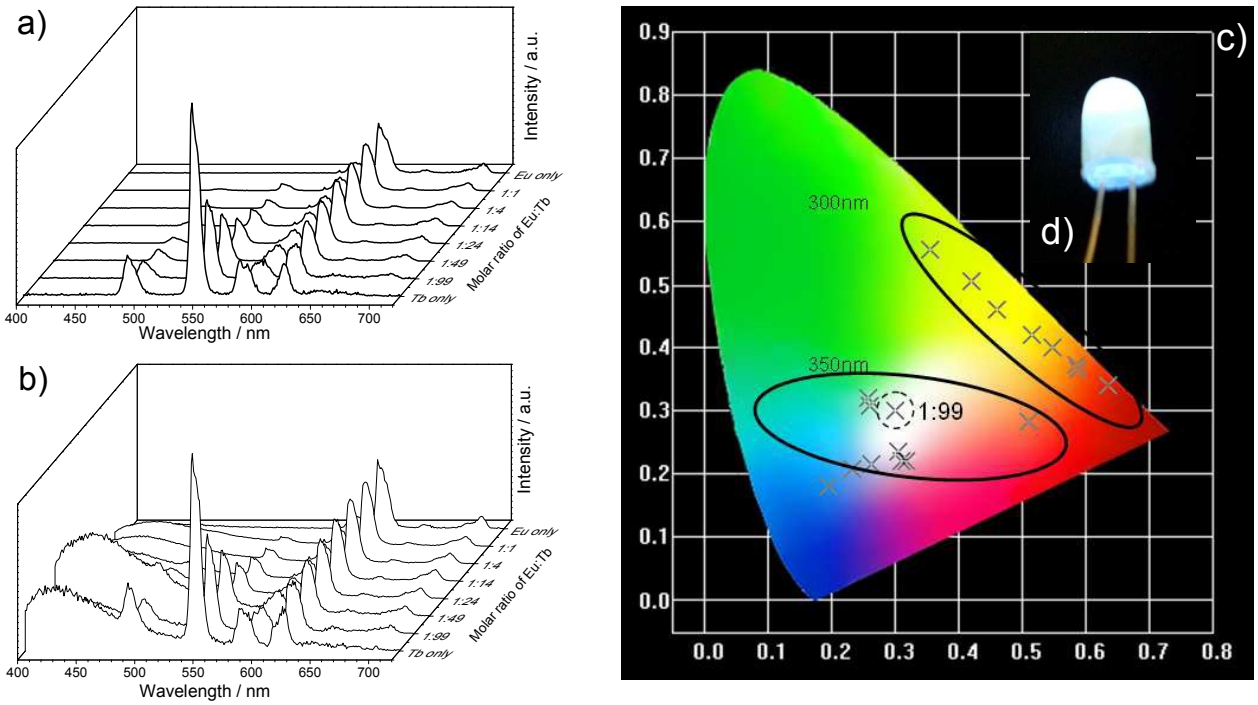

Figure 3. Emission spectra (normalized at 620nm) of the AC-Bipy-Ln (powder) excited at 300 (a) and 350 nm (b) and the CIE 1931 chromaticity diagram within the co-ordinates of AC-Bipy-Ln (powder) excited at various wavelength (c) within an image of 365 nm UV-LED cell (0.06 W) coated with AC-Bipy-Eu_1Tb_{99} (d). (All spectra were measured at room temperature)

The lifetimes of Eu^{3+} for AC-Bipy-Eu and Tb^{3+} for AC-Bipy-Tb (τ_{Eu} and τ_{Tb}) is determined to be 0.47 and 1.04 ms, respectively, from the corresponding decay curves (shown in Figure S2a and Figure S2b, respectively). The value is higher than similar materials previously reported by us, where the aromatic carboxylic acid used as the sensitizer [29]. It has been well documented that Ln^{3+} emission highly depends on its coordinated or nearby water molecules owing to the radiationless deactivation of the $^5D_0$ excited state. We therefore estimated the number of water molecules coordinated to Ln^{3+} (n_w) based on the lifetime of $^5D_0$ state (Eu^{3+}) and emission spectrum of AC-Bipy-Eu by using the empirical equation: [32]

$$n_w = 1.11(k_{exp} - k_r - 0.31) \quad (1)$$

where k_{exp} is the reciprocal value of the $^5D_0$ lifetime (ms^{-1}) and k_r is the radiative probabilities (ms^{-1}). The value of k_r can be estimated as follow: [33]

$$k_r = \frac{A_{0-1}E_{0-1}}{S_{0-1}}\sum_{J}^{2,4}\frac{S_{0-J}}{E_{0-J}} \quad (2)$$

where A_{0-1} is Einstein's coefficient of spontaneous emission between the $^5D_0$ and the $^7F_1$ Stark levels, which is approximately 50 s^{-1}, and E_{0-J} and S_{0-J} are the energy and the integrated intensity of the $^5D_0 \rightarrow {}^7F_J$ (J = 2 and 4) transitions, respectively. The corresponding data are exhibited in Table S2 (Supporting Information). Therefore, the n_w can be assumed to be 2, as shown in Scheme 1a. We also calculated the n_w of AC-BTC-Eu reported previously by us using this method and listed it in Table S2. Obviously, the AC-BTC-Ln exhibit a little bit higher n_w value compared with AC-Bipy-Ln. Thus the reason why the lifetimes of this work are higher than that reported previously can be satisfactorily explained.

Furthermore, the lifetimes of $^5D_4$ state for Tb^{3+} in AC-Bipy-Eu_xTb_y were also measured and shown in Figure 4a. The values are not equal to that in pure Tb^{3+} complex (AC-Bipy-Tb), suggesting that the energy transfer process from Tb^{3+} to Eu^{3+} exists, and the energy transfer efficiency from Tb^{3+} to Eu^{3+} ($\eta_{Tb\rightarrow Eu}$) can be calculated by the following equation: [11, 12, 34]

$$\eta_{Tb\rightarrow Eu} = 1 - \frac{\tau_1}{\tau_0} \quad (3)$$

where the τ_0 and τ_1 is the $^5D_4$ lifetime of Tb^{3+} in AC-Bipy-Tb and AC-Bipy-Eu_xTb_y, respectively. As a result, we obtained the variation curve of $\eta_{Tb\rightarrow Eu}$ as shown in Figure 4b. The $\eta_{Tb\rightarrow Eu}$ curve declines prominently when y/x is 14. A reasonable explanation for this phenomenon is that the $\eta_{Tb\rightarrow Eu}$ is proportional to R^{-6}, where R is the average distance between Tb^{3+} and Eu^{3+}. [35] The R is increased with the molar ratio of Eu^{3+} reduced, leading to the decrease of $\eta_{Tb\rightarrow Eu}$.

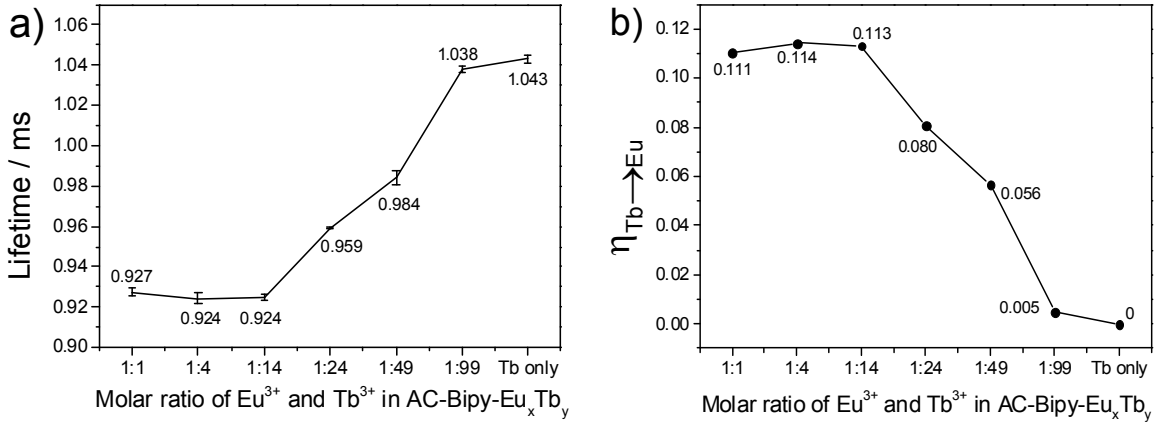

Figure 4. a) Variation curve of lifetimes of $^5D_4$ state for Tb^{3+} in AC-Bipy-Eu_xTb_y (λ_{ex} = 300 nm, $\lambda_{monitored}$ = 543 nm, all the lifetimes were measured for three times); b) variation curve of energy transfer efficiency from Tb^{3+} to Eu^{3+} in AC-Bipy-Eu_xTb_y ($\eta_{Tb\rightarrow Eu}$). These data were all obtained at room temperature.

Furthermore, the emission color of the hybrid materials highly depends on the excitation wavelength. As shown in Figure 3b, the emission spectra of the hybrid materials are composed of line-like bands attributed to f-f transition of Eu^{3+} and/or Tb^{3+} and a broad band ranging from 400 to 500 nm, the latter could be attributed to the emission of bipyridine moieties (Figure S1), when the hybrid materials were excited by a 350 nm wavelength. The CIE co-ordinates of AC-Bipy-Eu_xTb_y (λ_{ex} = 350 nm) were

shown in Figure 3c and Table S1. Remarkably, the AC-Bipy-Eu_1Tb_{99} has an excellent co-ordinate of (0.30, 0.30) located in the "white region" of CIE 1931 chromaticity diagram, which is very close to the ideal co-ordinate of white light (0.33, 0.33). We therefore coated the hydrogel of AC-Bipy-Eu_1Tb_{99} on a commercial available UV-LED cell and bright white light was obtained when the LED is on (Figure 3d). Compared with the formerly obtained white-light-emitting material, AC-BTC-Eu_1Tb_7, [29] the AC-Bipy-Eu_1Tb_{99} coated UV-LED cell has purer white light emission ascribed to its longer excitation wavelength (350 nm for AC-Bipy-Eu_1Tb_{99} and 325 nm for AC-BTC-Eu_1Tb_7).

Attributed to the temperature-dependent luminescent behavior as well as several advantages such as accurate, noninvasive, fast response and high sensitivity, [12, 36-39] such luminescent materials can be utilized as thermosensor. Theoretically, the emission intensity of the lanthanide complex is supposed to decrease upon increasing temperature ascribed to the thermal activation of nonradiative-decay channels. [40] Temperature-dependent emission spectra of AC-Bipy-Eu shown in Figure 5a and c were measured under 300 nm UV light excitation from 78 to 288 K (same as the AC-Bipy-Tb). The emission intensity of $^5D_0 \rightarrow {}^7F_2$ transition (614 nm) has no conspicuous change until T = 228 K (T = temperature) and then reduces linearly by about 0.55 % per K. This suggests that AC-Bipy-Eu is not very sensitive at low temperature (under 228 K). However, the AC-Bipy-Tb exhibits different temperature-dependent emission spectra (Figure 5b and c) compared with AC-Bipy-Eu. The emission intensity of $^5D_4 \rightarrow {}^7F_5$ transition (543 nm) keeps decreasing fast when the T is higher than 138 K and finally becomes extremely low at room temperature, indicating that the AC-Bipy-Tb is much more sensitive about temperature variation than AC-Bipy-Eu. The normalized intensity ratio of $^5D_4 \rightarrow {}^7F_5$ transition (AC-Bipy-Tb) to $^5D_0 \rightarrow {}^7F_2$ transition (AC-Bipy-Eu) (I_{Tb}/I_{Eu}) from 138 to 288 K can be linearly fitted as the following equation:

$$T = 296.71 - 153.85 * I_{Tb}/I_{Eu} \text{ (K)} \quad (4)$$

which is the equivalent transformation of the equation shown in Figure 5d, with a variation rate of 0.65 % per K and does not need any additional parameter. This is higher than that of our previously obtained AC-BTC-Eu_1Tb_7 [29] Such temperature-dependent emission spectra are repeatable and reversible. Thus we can use AC-Bipy-Eu and AC-Bipy-Tb simultaneously as self-referencing luminescent thermometer (138 to 288 K, excited at 300 nm).

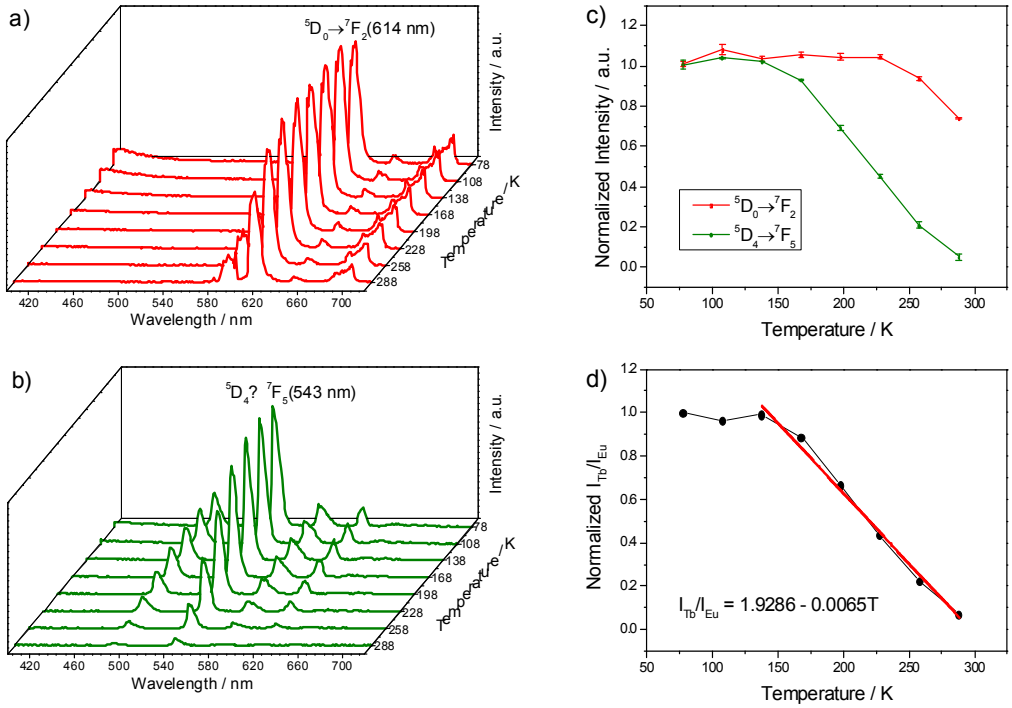

Figure 5. Temperature-dependent emission spectra of AC-Bipy-Eu (a) and AC-Bipy-Tb (b) excited at 300 nm; c) temperature dependence of normalized intensity of the $^5D_0 \rightarrow {}^7F_2$ transition (614 nm) for AC-Bipy-Eu (red curve) and $^5D_4 \rightarrow {}^7F_5$ transition (543 nm) for AC-Bipy-Tb (green curve). All the data were measured for three times; d) temperature dependence of the normalized intensity ratio of $^5D_4 \rightarrow {}^7F_5$ transition (AC-Bipy-Tb) to $^5D_0 \rightarrow {}^7F_2$ transition (AC-Bipy-Eu) from 138 to 288 K. The curve was linearly fitted (I_{Tb}/I_{Eu} = 1.9286 - 0.0065T, where T is the temperature, R^2 = 0.990).

Cite this: DOI: 10.1039/cOxxOOOOOx

www.rsc.org/xxxxxx

PAPER

Transparent luminescent thin films have also been successfully prepared by simply drop-casting the dilute hydrogels of AC-Bipy-Ln (about 1 % in mass ratio) onto 2 cm × 2 cm quartz substrate (Figure 6a) followed by dehydration at 40 ℃ in air. Figure 6b, Figure S3 and S4 present the luminescent performance of the thin films, and the CIE co-ordinates of which were also shown in Table S1. Similarly, the emission colors can be fine tuned by varying the molar ratio of Eu^{3+} and Tb^{3+} and the excitation wavelength. The films of AC-Bipy-Eu_1Tb_{24}, AC-Bipy-Eu_1Tb_{49} and AC-Bipy-Eu_1Tb_{99} are all able to emit white light under 350 nm UV light illumination, especially the AC-Bipy-Eu_1Tb_{24}, with a satisfied CIE co-ordinate of (0.32, 0.33). These luminescent thin films are possibly available for application in the fields of optoelectronics and sensing. [41, 42]

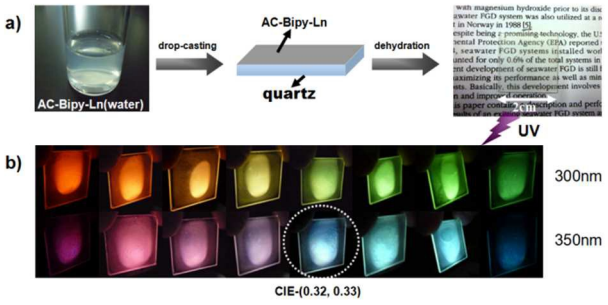

Figure 6. a) Preparation of the transparent luminescent thin films on quartz substrate; b) digital photographs of the thin films under 300 and 350 nm UV light irradiation (AC-Bipy-Eu, AC-Bipy-Eu_1Tb_1, AC-Bipy-Eu_1Tb_4, AC-Bipy-Eu_1Tb_{14}, AC-Bipy-Eu_1Tb_{24}, AC-Bipy-Eu_1Tb_{49}, AC-Bipy- Eu_1Tb_{99} and AC-Bipy-Tb, from left to right in the order, respectively).

Conclusions

In summary, we have successfully developed a novel kind of multicolored hybrid materials based on aminoclay, organic ligand and Ln^{3+} through a simple and green procedure, which exhibit bettered emission intensity and improved color purity compared with the AC-BTC-Ln that we obtained previously. Emission colors of the materials can be fine tuned by varying the molar ratio of Eu^{3+} and Tb^{3+}, excitation wavelength and temperature, and white light was obtained as well. On the other hand, the different temperature-dependent luminescent behavior between AC-Bipy-Eu and AC-Bipy-Tb affords them good candidates for self-referencing luminescent thermometers. Moreover, the excellent water processibility of the materials enables them to be fabricated as transparent thin films on quartz substrate or be coated on the round-shaped UV-LED cell, making them potentially available for designing optoelectronic devices.

Experimental Section

Materials

3-aminopropyltriethoxysilane (APTES, Aldrich, 99 %), $MgCl_2·6H_2O$ (CP), 2,2'-Bi-pyridine-4,4'-dicarboxylic acid (H_2Bipydc, Aldrich, 97 %), Eu_2O_3 (99.99 %) and Tb_4O_7 (99.99 %) were used as received. Aminoclay (AC) was synthesized through the previous reported procedure. [29] 0.05 mol·L^{-1} Na_2Bipydc aqueous solution was obtained by dissolving H_2Bipydc into 0.5 mol·L^{-1} NaOH aqueous solution. 0.1 mol·L^{-1} $EuCl_3$ aqueous solution and 0.1 mol·L^{-1} $TbCl_3$ aqueous solution were obtained by dissolving Eu_2O_3 and Tb_4O_7 into concentrated hydrochloric acid (37 %), respectively.

Characterization

The solid-state luminescence spectra and the lifetimes were measured on an Edinburgh Instrument FS920P spectrometer, with a 450 W xenon lamp as the steady-state excitation source, a double excitation monochromator (1800 lines mm^{-1}), an emission monochromator (600 lines mm^{-1}), a semiconductor cooled Hamamatsu RMP928 photomultiplier tube. Powder samples and films on quartz substrate were directly put in the chamber of the instrument, for the phtotophysical measurements. A microsecond flash lamp (pulse length: 2 μs) was used as the excitation source for the lifetime measurements. Photons were collected up to 10 ms until maximum of 104 counts. Decay curves were fitted according to the single-exponential function ($I = I_0 + A * exp(-(t-t_0) / \tau)$). The OptistatDN2 liquid nitrogen cryostat was used for the measurement of the temperature-dependent luminescence spectra.

Acknowledgements

Financial support by the National Key Basic Research Program (2012CB626804), the National Natural Science Foundation of China (20901022, 21171046, 21271060, and 21236001), the Tianjin Natural Science Foundation (13JCYBJC18400), the Natural Science Foundation of Hebei Province (No. B2013202243), the Program for Changjiang Scholars and Innovative Research Team in University (PCSIRT, IRT1059), and Educational Committee of Hebei Province (2011141, LJRC021) is gratefully acknowledged.

Notes and references

School of Chemical Engineering and Technology, Hebei University of Technology, Tianjin, 300130, P. R. China. E-mail: lihuanrong@hebut.edu.cn

† Electronic Supplementary Information (ESI) available: [Emission spectra as well as digital photograph of AC-Bipy, decay curves of $^5D_0$ state for Eu^{3+} in AC-Bipy-Eu and $^5D_4$ state for Tb^{3+} in AC-Bipy-Tb, emission spectra of the luminescent films on quartz, CIE 1931 chromaticity diagram within the co-ordinates of the luminescent films on quartz, CIE co-ordinates of the materials and photophysical data of AC-Bipy-Eu and AC-BTC-Eu]. See DOI: 10.1039/b000000x/

References

1. Y. Wada, M. Sato and Y. Tsukahara, *Angew. Chem. Int. Ed.*, 2006, **45**, 1925-1928.
2. D. Zhao, S. J. Seo and B. S. Bae, *Adv. Mater.*, 2007, **19**, 3473-3479.
3. P. Coppo, M. Duati, V. N. Kozhevnikov, J. W. Hofstraat and L. De Cola, *Angew. Chem.*, 2005, **117**, 1840-1844.
4. G. He, D. Guo, C. He, X. Zhang, X. Zhao and C. Duan, *Angew. Chem. Int. Ed.*, 2009, **48**, 6132-6135.
5. H. Zhang, X. Shan, L. Zhou, P. Lin, R. Li, E. Ma, X. Guo and S. Du, *J. Mater. Chem. C*, 2013, **1**, 888-891.
6. J. Leng, H. Li, P. Chen, W. Sun, T. Gao and P. Yan, *Dalton Trans.*, 2014.
7. J. Feng and H. Zhang, *Chem. Soc. Rev.*, 2013, **42**, 387-410.
8. J. Massue, S. J. Quinn and T. Gunnlaugsson, *J. Am. Chem. Soc.*, 2008, **130**, 6900-6901.
9. L. D. Carlos, R. A. Ferreira, V. d. Z. Bermudez and S. J. Ribeiro, *Adv. Mater.*, 2009, **21**, 509-534.
10. J. Cuan and B. Yan, *RSC Adv.*, 2013, **3**, 20077-20084.
11. K. Miyata, Y. Konno, T. Nakanishi, A. Kobayashi, M. Kato, K. Fushimi and Y. Hasegawa, *Angew. Chem.*, 2013, **125**, 6541-6544.
12. X. Rao, T. Song, J. Gao, Y. Cui, Y. Yang, C. Wu, B. Chen and G. Qian, *J. Am. Chem. Soc.*, 2013, **135**, 15559-15564.
13. K. Binnemans, *Chem. Rev.*, 2009, **109**, 4283-4374.
14. P. Li, Y. Wang, H. Li and G. Calzaferri, *Angew. Chem. Int. Ed.*, 2014, **53**, 2904-2909.
15. D. K. Sendor, L., *Adv. Mater.*, 2002, **14**, 1570-1574.
16. E. H. de Faria, E. J. Nassar, K. J. Ciuffi, M. A. Vicente, R. Trujillano, V. Rives and P. S. Calefi, *ACS Appl. Mater. Interfaces*, 2011, **3**, 1311-1318.
17. H. R. Silva, M. G. Fonseca, J. G. P. Espínola, H. F. Brito, W. M. Faustino and E. E. Teotonio, *Eur. J. Inorg. Chem.*, 2014, **2014**, 1914-1921.
18. Y. Ma, H. Wang, W. Liu, Q. Wang, J. Xu and Y. Tang, *J. Phys. Chem. B*, 2009, **113**, 14139-14145.
19. X. Chen, P. Zhang, T. Wang and H. Li, *Chem. Eur. J.*, 2014, **20**, 2551-2556.
20. S. Marchesi, F. Carniato and E. Boccaleri, *New J. Chem.*, 2014, **38**, 2480-2485.
21. K. Binnemans, *Chem. Rev.*, 2007, **107**, 2592-2614.
22. Q. Ru, Z. Xue, Y. Wang, Y. Liu and H. Li, *Eur. J. Inorg. Chem.*, 2014, **2014**, 469-474.
23. P. R. Matthes, C. J. Holler, M. Mai, J. Heck, S. J. Sedlmaier, S. Schmiechen, C. Feldmann, W. Schnick and K. Muller-Buschbaum, *J. Mater. Chem.*, 2012, **22**, 10179-10187.
24. L. V. Meyer, F. Schonfeld and K. Muller-Buschbaum, *Chem. Commun.*, 2014, **50**, 8093-8108.
25. T.-W. Duan and B. Yan, *J. Mater. Chem. C*, 2014, **2**, 5098-5104.
26. K. V. Rao, A. Jain and S. J. George, *J. Mater. Chem. C*, 2014, **2**, 3055-3064.
27. K. V. Rao, K. Datta, M. Eswaramoorthy and S. J. George, *Adv. Mater.*, 2013, **25**, 1713-1718.
28. K. V. Rao, K. Datta, M. Eswaramoorthy and S. J. George, *Angew. Chem. Int. Ed.*, 2011, **50**, 1179-1184.
29. T. Wang, P. Li and H. Li, *ACS Appl. Mater. Interfaces*, 2014.
30. P. S. Calefi, A. O. Ribeiro, A. M. Pires and O. A. Serra, *J. Alloy Comp.*, 2002, **344**, 285-288.
31. H. Li, J. Yu, F. Liu, H. Zhang, L. Fu, Q. Meng, C. Peng and J. Lin, *New J. Chem.*, 2004, **28**, 1137-1141.
32. R. M. Supkowski and W. D. Horrocks Jr, *Inorg. Chim. Acta*, 2002, ***340***, 44-48.
33. M. H. Werts, R. T. Jukes and J. W. Verhoeven, *Phys. Chem. Chem. Phys.*, 2002, **4**, 1542-1548.
34. Y. Cui, H. Xu, Y. Yue, Z. Guo, J. Yu, Z. Chen, J. Gao, Y. Yang, G. Qian and B. Chen, *J. Am. Chem. Soc.*, 2012, **134**, 3979-3982.
35. M. Shang, G. Li, X. Kang, D. Yang, D. Geng and J. Lin, *ACS Appl. Mater. Interfaces*, 2011, **3**, 2738-2746.
36. H. Peng, M. I. Stich, J. Yu, L. n. Sun, L. H. Fischer and O. S. Wolfbeis, *Adv. Mater.*, 2010, **22**, 716-719.
37. C. D. Brites, P. P. Lima, N. J. Silva, A. Millán, V. S. Amaral, F. Palacio and L. D. Carlos, *Adv. Mater.*, 2010, **22**, 4499-4504.
38. C. D. Brites, P. P. Lima, N. J. Silva, A. Millán, V. S. Amaral, F. Palacio and L. D. Carlos, *Nanoscale*, 2012, **4**, 4799-4829.
39. X.-d. Wang, O. S. Wolfbeis and R. J. Meier, *Chem. Soc. Rev.*, 2013, **42**, 7834-7869.
40. M. Bhaumik, *The J. Chem. Phys.*, 1964, **40**, 3711-3715.
41. Y. Wang, H. Li, Y. Feng, H. Zhang, G. Calzaferri and T. Ren, *Angew. Chem. Int. Ed.*, 2010, **49**, 1434-1438.
42. P. Cao, Y. Wang, H. Li and X. Yu, *J. Mater. Chem.*, 2011, **21**, 2709-2714.